



## Regular article

## Pure climb of [001] dislocations in TiAl at 850 °C

Soumaya Naanani<sup>a,b</sup>, Jean-Philippe Monchoux<sup>a</sup>, Catherine Mabru<sup>b</sup>, Alain Couret<sup>a,\*</sup><sup>a</sup> CEMES, Université de Toulouse, CNRS, 29 rue Jeanne Marvig, 31055 Toulouse, France<sup>b</sup> ICA, Université de Toulouse, CNRS, 3 rue Caroline Aigle, 31400 Toulouse, France

## ARTICLE INFO

## Article history:

Received 15 December 2017

Received in revised form 1 February 2018

Accepted 1 February 2018

Available online xxxx

## Keywords:

Titanium aluminides

High-temperature deformation

Transmission electron microscopy

Plasticity

Dislocation climb

## ABSTRACT

This paper presents a study by Transmission Electron Microscopy of the deformation microstructure in the  $\gamma$  phase of a TiAl alloy crept at 850 °C under 150 MPa. A never observed population of dislocations is evidenced and characterized. It is shown that their Burgers vector is of [001] type and that they are moving by pure climb in the (001) planes. The reasons of the presence of these dislocations are discussed.

© 2018 Acta Materialia Inc. Published by Elsevier Ltd. All rights reserved.

Although TiAl alloys are candidate to be used at temperatures higher than 800 °C in aeronautic and automotive engines, the deformation mechanisms activated in this temperature range in industrial alloys with complex microstructures are still not really understood. The few studies reported in literature on the deformation of TiAl alloys at high temperatures all agree to attribute the deformation mainly to twinning and ordinary dislocations [1,2] and more scarcely to [001] and  $\langle 100 \rangle$  dislocations [3–5] and  $\langle 011 \rangle$  and  $1/2 \langle 112 \rangle$  superlattice dislocations [6]. For the case of ordinary dislocations, glide configurations characterized by dislocation elongation along their screw direction and by numerous pinning points are still observed at 900 °C [2]. In aluminum rich single crystals, Inui et al. have noted the glide of these ordinary dislocations in non-compact planes, as (001) and (110) planes [7]. However, a contribution of climb has been evidenced in several contributions [2,7,8] and associated to the transition between the brittle to ductile material behavior [1,2,5,8]. Interestingly, Kad and Fraser have shown that a decrease of the strain rate promotes the activation of climb instead of glide [2]. They have proposed that at low strain rates, climb is activated in a second step when an appropriated density of dislocations has been previously created by glide. Following the simultaneous observations of glide and climb dislocations in samples crept at 700 °C, the activation in some grains of a high density of gliding dislocations similar to that observed at intermediate temperatures has been ascribed to the accommodation of high local internal stresses [9]. From *in situ* heating experiments, climbing ordinary dislocations are seen to be preferentially oriented along the  $\langle 110 \rangle$  orientations and forming helicoidal structure [8,10,11]. Malaplate et al. [10] has demonstrated that during creep

at 700 °C, these ordinary dislocations can move by a mixed climb mechanism which is a mixture of glide and climb and which may explain the high measured values of the activation volume, previously underlined by Appel et al. [8]. The [001] dislocations have been observed to glide in {110} planes in single crystals at 950 °C under favorable orientation conditions [3] and lying in pile-ups at 1000 °C in an aluminum rich alloy [5].

In this context, the present study aims at analyzing the dislocations microstructure and at determining the activated deformation mechanisms in an industrial TiAl alloy exhibiting a complex microstructure and crept at 850 °C. Here, observations and characterizations of a population of dislocations are reported, which, in our knowledge, has never been described in the current literature. The reason of the activation of this new type of dislocations will be discussed in the final section.

The alloy investigated is an IRIS alloy (Ti – 48Al – 2W – 0.08B) obtained by the densification of a pre-alloyed powder by Spark Plasma Sintering [12]. Its microstructure is formed by small lamellar grains surrounded by borders made of single phased  $\gamma$  grains that contain B2 precipitates [13]. The alloy was crept at 850 °C under 150 MPa up to 1.5% of strain. Under this sollicitation, the minimum creep rate was  $6 \cdot 10^{-8} \text{ s}^{-1}$  and the creep life was 260 h. Thin foils suitable for Transmission Electron Microscopy (TEM) were extracted from this crept sample with their planes cut perpendicular to the tensile axis of the sample. They were examined in a JEOL 2010 TEM using a Tilt-Rotation specimen holder commercialized by the Gatan company, with the aim to obtain observations under various diffracting conditions. This holder allows the following movements of the specimen: (i) a 360° rotation around the direction of the electron beam, which is perpendicular to the thin foil plane at zero tilt and (ii) the usual tilt  $\pm 40^\circ$  around the longitudinal tilt axis of TEM holders, which is situated along the vertical direction on

\* Corresponding author.

E-mail address: [alain.couret@cemes.fr](mailto:alain.couret@cemes.fr) (A. Couret).

all the micrographs presented in this report. As usual for the  $\gamma$  phase of TiAl alloys, the quadratic  $L1_0$  structure will be treated as an ordered face-centered cubic structure consistently with a  $c/a$  ratio close to 1.

Fig. 1 displays the deformation microstructure in a  $\gamma$  grain of a border using the  $\mathbf{g} = (\bar{1}\bar{1}1)$  reflection ( $\mathbf{g}$  is the vector of the reciprocal lattice normal to the plane used to obtain the image in two beams condition;  $\mathbf{g}$  is called the diffracting vector in what follows). This microstructure consists of nearly rectilinear dislocations, which appear to be elongated along directions situated at  $45^\circ$  from each other. No pinning points generally observed on gliding ordinary dislocations [14–16] are seen on these dislocations. Fig. 1,b shows the stereographic projection of this grain under zero tilt. The perpendicular to the thin foil plane (T), which is also the direction of the loading axis is at  $22^\circ$  of the  $[001]$  direction. The deformation microstructure has been studied in ten  $\gamma$  grains of the borders by TEM, and in three of them such kind of rectilinear dislocations has been observed. In Fig. 2, the dislocation loop situated in the red rectangle marked on Fig. 1 is observed under different diffracting conditions. The loop is visible with three reflections of the  $\langle 111 \rangle$  type. This indicates that the Burgers vector is neither that of an ordinary dislocation ( $1/2 < 110 \rangle$  type), nor that of a superdislocation of  $\langle 101 \rangle$  type.

For the micrographs of Fig. 3, the (001) plane is perpendicular to the electron beam (a) and the  $\mathbf{g}$  diffracting vectors are all perpendicular to the  $[001]$  direction; two of them are of  $\langle 200 \rangle$  type and the two others of the  $\langle 220 \rangle$  one. The rectilinear segments are parallel to the projections of the  $\langle 100 \rangle$  and  $\langle 110 \rangle$  directions of the crystal. Remarkably, as surrounded red, on each of these micrographs one segment is not visible contrary to the others. Moreover, these invisible segments appear to be parallel to the direction of the corresponding  $\mathbf{g}$  diffracting vector. This kind of contrast is known to exist for the case of edge dislocations while the  $\mathbf{g}\mathbf{b} = 0$  extinction condition is fulfilled [17,18], as exemplified in the complex metallic alloy  $\xi$  - Al - Pd - Mn [19]. In this configuration, complete invisibility is only obtained if a second condition extinction  $\mathbf{g}\mathbf{b}\mathbf{u} = 0$

is also fulfilled ( $\mathbf{u}$  is the unit vector along the dislocation line). If it is not, strong residual contrasts are observed, particularly when  $\mathbf{g}\mathbf{b}\mathbf{u} > 0.6$  [17,18]. This kind of residual contrast results from the bugling by edge dislocations of the diffracting plane, which is perpendicular to the extra half plane and contains the Burgers vector (see Fig. 25.4 of [18]).

To explain all these TEM observations, the only solution is to have the Burgers vector of this dislocation parallel to the  $[001]$  direction ( $\mathbf{b} = [001]$ ), which is perpendicular to all the used diffracting vectors ( $\mathbf{g}\mathbf{b} = 0$ ). Considering the situation depicted by the Fig. 3,  $\mathbf{b} (\mathbf{g} = [200])$ , three situations are encountered:

- when  $\mathbf{u} // \mathbf{g} // [200]$ ,  $\mathbf{b}\mathbf{u}$  will be perpendicular to  $\mathbf{g}$ , the scalar product of  $\mathbf{g}$  by  $\mathbf{b}\mathbf{u}$  is equal to 0 and the dislocation will be invisible. That is the case of the red arrowed segment.
- when  $\mathbf{u} // [020]$  and  $\perp$  to  $\mathbf{g} = [200]$ ,  $\mathbf{b}\mathbf{u}$  will be parallel to  $\mathbf{g}$ , the scalar product of  $\mathbf{g}$  by  $\mathbf{b}\mathbf{u}$  is different of 0 and is in fact equal to  $\pm 2$ . The dislocation segment is visible, due to a strong residual contrast.
- when  $\mathbf{u} // [220]$  or  $[2\bar{2}0]$ , the scalar product of  $\mathbf{g}$  by  $\mathbf{b}\mathbf{u}$  is different of 0 and equal to  $\pm\sqrt{2}$ . The dislocation is visible.

The three other situations of Fig. 3, c-e can be analyzed in the same way.

As a conclusion, all the TEM experimental observations are explained by considering that the dislocation loop is made of  $[001]$  dislocations which are pure edge in character and lying along the  $\langle 100 \rangle$  and  $\langle 110 \rangle$  directions.

To determine the plane in which these dislocations are moving, tilt experiments have been performed around various directions. Fig. 4 presents one of them, for which, using the holder rotation, the normal to the (001) plane has been placed perpendicular to the tilt axis. It follows that the trace of this (001) plane is going through this tilt axis and stays

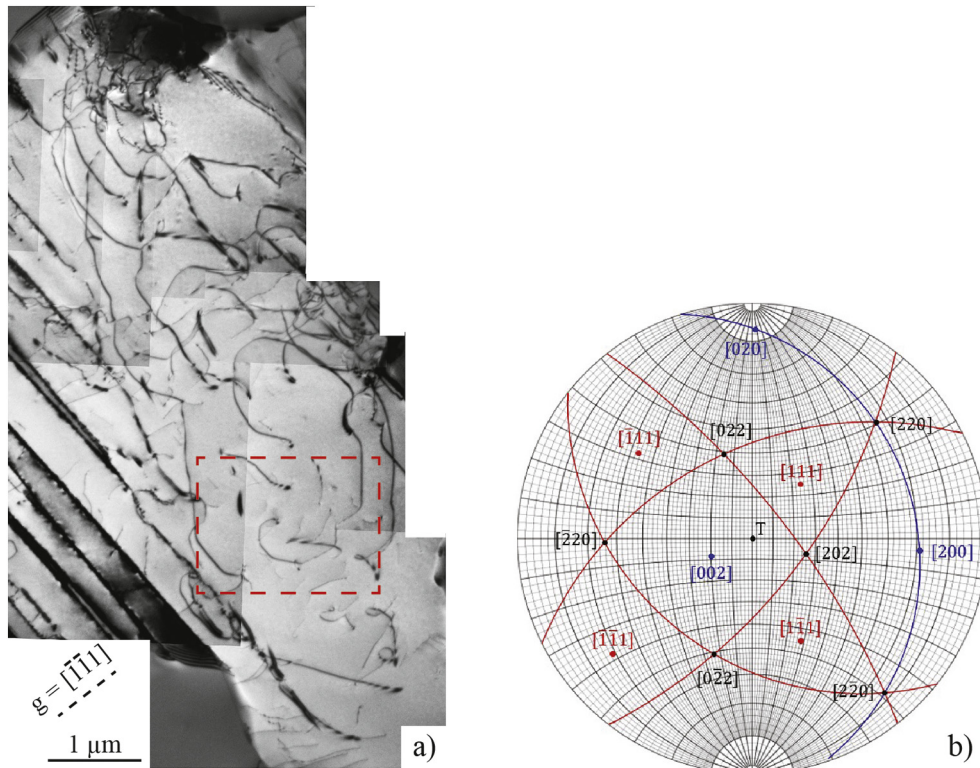


Fig. 1. General view (a) and stereographic projection (b) of the  $\gamma$  grain investigated in the present study. On (b), the poles of the plane are labelled by their direction in the reciprocal lattice, T is the direction of the tensile axis of the crept sample.

Download English Version:

<https://daneshyari.com/en/article/7910924>

Download Persian Version:

<https://daneshyari.com/article/7910924>

[Daneshyari.com](https://daneshyari.com)